

ORIGINAL ARTICLE

Open Access



^{18}F -fluorothymidine (FLT)-PET and diffusion-weighted MRI for early response evaluation in patients with small cell lung cancer: a pilot study

Tine Nøhr Christensen^{1,2*} , Seppo W. Langer³, Katrine Engholm Villumsen¹, Helle Hjorth Johannesen¹, Johan Löfgren¹, Sune Høgdild Keller¹, Adam Espe Hansen¹, Andreas Kjaer^{1,2} and Barbara Malene Fischer^{1,4}

* Correspondence: tine.noehr.christensen.02@regionh.dk

¹Department of Clinical Physiology, Nuclear Medicine & PET, Rigshospitalet, University of Copenhagen, Blegdamsvej 9, 2100 Copenhagen Ø, Denmark

²Cluster for Molecular Imaging, University of Copenhagen, Copenhagen, Denmark

Full list of author information is available at the end of the article

Abstract

Background: Small cell lung cancer (SCLC) is an aggressive cancer often presenting in an advanced stage and prognosis is poor. Early response evaluation may have impact on the treatment strategy.

Aim: We evaluated ^{18}F -fluorothymidine-(FLT)-PET/diffusion-weighted-(DW)-MRI early after treatment start to describe biological changes during therapy, the potential of early response evaluation, and the added value of FLT-PET/DW-MRI.

Methods: Patients with SCLC referred for standard chemotherapy were eligible. FLT-PET/DW-MRI of the chest and brain was acquired within 14 days after treatment start. FLT-PET/DW-MRI was compared with pretreatment FDG-PET/CT. Standardized uptake value (SUV), apparent diffusion coefficient (ADC), and functional tumor volumes were measured. $\text{FDG-SUV}_{\text{peak}}$, $\text{FLT-SUV}_{\text{peak}}$ and $\text{ADC}_{\text{median}}$; spatial distribution of aggressive areas; and voxel-by-voxel analyses were evaluated to compare the biological information derived from the three functional imaging modalities. $\text{FDG-SUV}_{\text{peak}}$, $\text{FLT-SUV}_{\text{peak}}$ and $\text{ADC}_{\text{median}}$ were also analyzed for ability to predict final treatment response.

Results: Twelve patients with SCLC completed FLT-PET/MRI 1–9 days after treatment start. In nine patients, pretreatment FDG-PET/CT was available for comparison. A total of 16 T-sites and 12 N-sites were identified. No brain metastases were detected. $\text{FDG-SUV}_{\text{peak}}$ was 2.0–22.7 in T-sites and 5.5–17.3 in N-sites. $\text{FLT-SUV}_{\text{peak}}$ was 0.6–11.5 in T-sites and 1.2–2.4 in N-sites. $\text{ADC}_{\text{median}}$ was $0.76\text{--}1.74 \times 10^{-3} \text{ mm}^2/\text{s}$ in T-sites and $0.88\text{--}2.09 \times 10^{-3} \text{ mm}^2/\text{s}$ in N-sites. $\text{FLT-SUV}_{\text{peak}}$ correlated with $\text{FDG-SUV}_{\text{peak}}$ and voxel-by-voxel correlation was positive, though the hottest regions were dissimilarly distributed in FLT-PET compared to FDG-PET. $\text{FLT-SUV}_{\text{peak}}$ was not correlated with $\text{ADC}_{\text{median}}$ and voxel-by-voxel analyses and spatial distribution of aggressive areas varied with no systematic relation. $\text{FLT-SUV}_{\text{peak}}$ was significantly lower in responding lesions than non-responding lesions (mean $\text{FLT-SUV}_{\text{peak}}$ in T-sites: 1.5 vs. 5.7; $p = 0.007$, mean $\text{FLT-SUV}_{\text{peak}}$ in N-sites: 1.6 vs. 2.2; $p = 0.013$).

Conclusions: FLT-PET and DW-MRI performed early after treatment start may add biological information in patients with SCLC. Proliferation early after treatment start measured by FLT-PET is a promising predictor for final treatment response that warrants further investigation.

(Continued on next page)

(Continued from previous page)

Trial registration: Clinicaltrials.gov, [NCT02995902](https://clinicaltrials.gov/ct2/show/study/NCT02995902). Registered 11 December 2014 - Retrospectively registered.

Keywords: Small cell lung cancer, SCLC, FLT-PET, ¹⁸F-fluorothymidine, PET/MRI, Diffusion-weighted MRI, DW-MRI, Early treatment evaluation, Response evaluation, Prediction of response

Introduction

Functional imaging, such as positron emission tomography (PET) and diffusion-weighted magnetic resonance imaging (DW-MRI), are important tools to gain non-invasive information about tumor biology and tumor heterogeneity. ¹⁸F-fluorodeoxy-glucose (FDG)-PET/CT has established its role in staging of small cell lung cancer (SCLC) (Ruben and Ball 2012) and causes stage migration in up to 40% of the patients influencing the choice of treatment and outcome (van Loon et al. 2011). FDG-PET has shown prognostic value in SCLC (Langer et al. 2014; Lee et al. 2014; Park et al. 2014; Aktan et al. 2017; Kim et al. 2018; Mirili et al. 2019; Fu et al. 2018; Chang et al. 2019), but the potential of FDG-PET for early response evaluation remains unclear (Yamamoto et al. 2009; Fischer et al. 2006).

SCLC is an aggressive cancer with more than two-thirds of the patients presenting in stage IV (Dayen et al. 2017). Over the last three decades, improvements for patients with SCLC have been sparse. However recently, new drug classes including immune check point inhibitors (Ready et al. 2018; Horn et al. 2018) and transcription inhibitors (Luis et al. 2019) have raised hope for improving the treatment results. Accordingly, the need for a better understanding of tumor biology and prognostication is higher than ever.

¹⁸F-fluorothymidine (FLT) is a PET-tracer of proliferation (Yap et al. 2006; Brockenbrough et al. 2011). FLT-PET has been studied in SCLC xenografts in mice showing promise for early response evaluation of treatment with epidermal growth factor receptor tyrosine kinase inhibitors (EGFR TKI) (Pardo et al. 2009), but we are unaware of any studies of FLT-PET in patients with SCLC. In patients with non-small cell lung cancer (NSCLC), pretreatment FLT-PET/CT and FLT-PET/CT early after treatment start has shown prognostic value (Yap et al. 2006; Brockenbrough et al. 2011; Usuda et al. 2018; Kahraman et al. 2012; Trigonis et al. 2014). Early response evaluation measured by FLT-PET/CT was prognostic for progression-free survival (PFS) in patients with NSCLC treated with EGFR TKI (Kahraman et al. 2011; Mileschkin et al. 2011; Sohn et al. 2008). Results from patients treated with a platin-based chemotherapy (Crandall et al. 2017) and concurrent chemo-radiotherapy were, however, non-significant (Trigonis et al. 2014; Everitt et al. 2017). In contrary to FDG, FLT does not cross the blood-brain barrier if intact (Nikaki et al. 2017). FLT-PET is however able to detect brain tumors (Nikaki et al. 2017) and brain metastases (Nguyen et al. 2018; Dittmann et al. 2003; Nakajo et al. 2013; Hoshikawa et al. 2013) possible due to disruption of the blood brain-barrier in these patients.

DW-MRI measures water diffusion within the tissue which is affected by micro textural features. Tumors with a high cell density and a poor differentiation have restricted water diffusion, which can be quantified by a lower apparent diffusion coefficient (ADC) (Weiss et al. 2016). A meta-analysis has shown that ADC can distinguish

malignant lesions in the lungs from benign lesions and that ADC is lower in SCLC than NSCLC (Shen et al. 2016). ADC change after therapy has proven prognostic of overall survival (OS) in a study mixed of patients with SCLC and NSCLC (Tsuchida et al. 2013). Other studies of patients with NSCLC have confirmed predictive and prognostic value of ADC change during therapy (Weiss et al. 2016; Yabuuchi et al. 2011; Yu et al. 2014), though baseline ADC did not show prognostic value (Usuda et al. 2018; Yu et al. 2014).

The objectives of this study were to pilot the potential of FLT-PET and DWI-MRI early after treatment start in patients with SCLC; for early evaluation of tumor biology during treatment and for early response evaluation.

To our knowledge, this is the first study to examine FLT-PET in patients with SCLC.

Methods

Patients

Patients with histologically verified SCLC, referred to first line standard chemotherapy, and patients with relapsed SCLC referred to reinduction of standard chemotherapy, were eligible. Patients were recruited at the Dept. of Oncology, Rigshospitalet, Denmark from November 2014 to May 2017. All patients gave informed consent, and the study was approved by the local ethics committee, approval number H-1-2014-026.

Imaging

FLT-PET/MRI was performed within 14 days after start of chemotherapy on an integrated PET/MRI system (Siemens Biograph mMR) with a 3-T magnet. FLT (5 MBq/kg, max 350 MBq) was injected 60 min prior to PET/MRI, without restrictions regarding fasting or resting. PET and MRI were conducted simultaneously as static, regional images starting with one bed position over cerebrum followed by one bed position over thorax centered on the primary tumor. T1-weighted imaging with and without gadolinium contrast, T2-weighted imaging, and DWI were acquired over both bed positions using the following protocol:

Cerebrum: 3D VIBE for PET attenuation correction (echo time (TE) 4.00 ms; repetition time (TR) 8.6 ms; voxel size $1.1 \times 1.0 \times 7.0 \text{ mm}^3$); sagittal T1 MPRAGE (TE 2.44 ms; TR 1900 ms; voxel size $1.0 \times 1.0 \times 1.0 \text{ mm}^3$); transverse T2 BLADE (TE 117 ms; TR 5550 ms; voxel size $0.7 \times 0.7 \times 5.0 \text{ mm}^3$); DWI using single-shot echo-planar imaging (EPI) (TE 101 ms; TR 6800 ms; voxel size $1.1 \times 1.1 \times 4.0 \text{ mm}^3$, b values of 0 and 800 s/mm^2). Thorax: 3D VIBE for PET attenuation correction (TE 1.23/2.46 ms; TR 3.60 ms; voxel size $4.1 \times 2.6 \times 3.1 \text{ mm}^3$); transverse T1 VIBE in breath-hold (TE 1.23 ms; TR 3.46 ms; voxel size $1.7 \times 1.3 \times 4.0 \text{ mm}^3$); DWI using single-shot EPI triggered to the position of the diaphragm (TE 73 ms; TR 2200 ms; voxel size $3.7 \times 3.0 \times 5.0 \text{ mm}^3$; b values of 0, 150, 400, and 800 s/mm^2); coronal T2 BLADE in four breath-holds with Gadolinium-based contrast (TE 138 ms; TR 2030 ms; voxel size $1.4 \times 1.4 \times 6.0 \text{ mm}^3$); transverse T1 VIBE in breath-hold employing a small shim volume covering the tumor, with Gadolinium-based contrast (TE 1.23 ms; TR 3.46 ms; voxel size $1.7 \times 1.3 \times 4.0 \text{ mm}^3$). Cerebrum: sagittal T1 MPRAGE with Gadolinium-based contrast (TE 2.44 ms; TR 1900 ms; voxel size $1.0 \times 1.0 \times 1.0 \text{ mm}^3$).

FLT-PET data were reconstructed using ordinary Poisson 3D ordered subset expectation maximization (OP-OSEM) with three iterations, 21 subsets, voxel size $2.1 \times 2.1 \times 2.0 \text{ mm}^3$ with Siemens standard MR-based Dixon attenuation correction, and 4 mm post-filtering.

If pretreatment FDG-PET/CT had been performed, this was included in the study. Pretreatment FDG-PET/CT was at different hospitals by clinical indication. Accordingly, pretreatment FDG-PET/CT was performed on different scanner models and variant PET-protocols (details available in Additional file 1: Table S1).

Image analysis

All imaging datasets were analyzed on a Mirada Medical Ltd. XD 3.6 workstation (MIRADA Medical, Oxford, UK).

Metabolic tumor volume (MTV) was delineated on pretreatment FDG-PETs by thresholds of 41% and 50% of maximum standardized uptake value (SUV_{max}) (MTV41 and MTV50), as recommended by the European Association of Nuclear Medicine (EANM) procedure guidelines (Boellaard et al. 2015).

Proliferative tumor volume (PTV) being the functional tumor volume by FLT-PET (equivalent to MTV by FDG-PET) was delineated on posttreatment FLT-PETs using the same thresholds as recommended for FDG-PET (PTV41 and PTV50) as well as with an absolute threshold of $\text{SUV} = 1.4$ (PTV1.4), as recommended by Thureau et al. (2013). Within the above tumor volumes, volume, SUV_{max} , SUV_{peak} , and SUV_{mean} were measured. Total lesion glycolysis (TLG) by FDG-PET and total lesion proliferation (TLP) by FLT-PET were calculated by multiplying MTV and PTV with the corresponding SUV_{mean} (e.g., $\text{TLG}_{41} = \text{MTV}_{41} \times \text{SUV}_{\text{mean}41}$; $\text{TLP}_{50} = \text{PTV}_{50} \times \text{SUV}_{\text{mean}50}$) for each tumor volume.

Diffusion-weighted tumor volume (DWTV25) was delineated on DW-MRIs ($b = 800 \text{ s/mm}^2$) using a threshold of 25% of maximum. DWTV25 was projected to the ADC-map for quantifying ADC_{mean} and $\text{ADC}_{\text{median}}$.

In addition, volumes of the primary tumor, lymph nodes, and distant metastases included in the MRI field of view were contoured by an experienced radiologist on T1-weighted MRI with gadolinium contrast, following recommendations for delineation of gross tumor volume (GTV) (Nestle et al. 2018). The MRI contours were projected to FDG-PET, FLT-PET, and the ADC-map for voxel-by-voxel analyses comparing the modalities. Image modalities were rigidly registered and subsequently resampled to identical voxel sizes. Voxel-by-voxel analysis was considered reasonable when the measured position of lesional landmarks in registered scans deviated by less than 10 mm in the direction of maximum displacement *and* if visual inspection indicated good overall alignment, or in lesions with no characteristic landmarks, good overall alignment by visual inspection. If visual inspection indicated adequate overall alignment, a maximum of 5 mm in the direction of maximum displacement was considered reasonable for voxel-by-voxel analysis.

Within each lesion, we spatially compared the most “aggressive” areas within the tumor defined by each scan modality. The most aggressive areas were defined as the area with highest metabolism or highest proliferation measured by FDG-PET and FLT-PET, respectively, and by DW-MRI as the areas with lowest diffusion. The most

aggressive areas were delineated on FDG-PET and FLT-PET using a threshold of 70% of SUV_{max} (MTV70; PTV70), and on DW-MRI ($b = 800 \text{ s/mm}^2$) using a threshold of 50% (DWTV50).

Overlap of MTV70 vs. PTV70 and PTV70 vs. DWTV50 were analyzed visually. Overlap were graded as no overlap, partial overlap (< 50% overlap), or high overlap (> 50% overlap).

As a quality control, FLT uptake within normal tissue was measured, as recommended by Cysouw et al. (2017). Briefly, liver FLT-uptake was measured in a 3-cm-diameter sphere placed in the right upper lobe of the liver; bone marrow FLT-uptake was measured in a 1-cm-diameter sphere placed in a lower thoracic vertebra; and FLT-uptake in the mediastinal blood pool was measured in a cylinder of $1 \times 2 \text{ cm}$ in ascending aorta. Metastases, previously irradiated tissue, and the aortic wall were avoided. Within these volumes, $FLT-SUV_{max}$, $FLT-SUV_{peak}$, and $FLT-SUV_{mean}$ were measured.

Follow up and outcome

Patients were followed until 1 year after the last patient had completed FLT-PET/MRI.

Final response to treatment was determined by routine CT using The Response Evaluation Criteria in Solid Tumors (RECIST) 1.1 (Eisenhauer et al. 2009).

Response of each lesion was defined by the same limits as used in RECIST 1.1 (response: > 30% decrease of longest lesion diameter; progression: > 20% increase of longest lesion diameter; no change: neither response nor progression).

PFS was defined as time from PET/MRI to progression or death of any cause, whichever occurred first. OS was defined as time from PET/MRI to death of any cause.

Statistics

Statistical analyses were performed in SPSS, version 25.

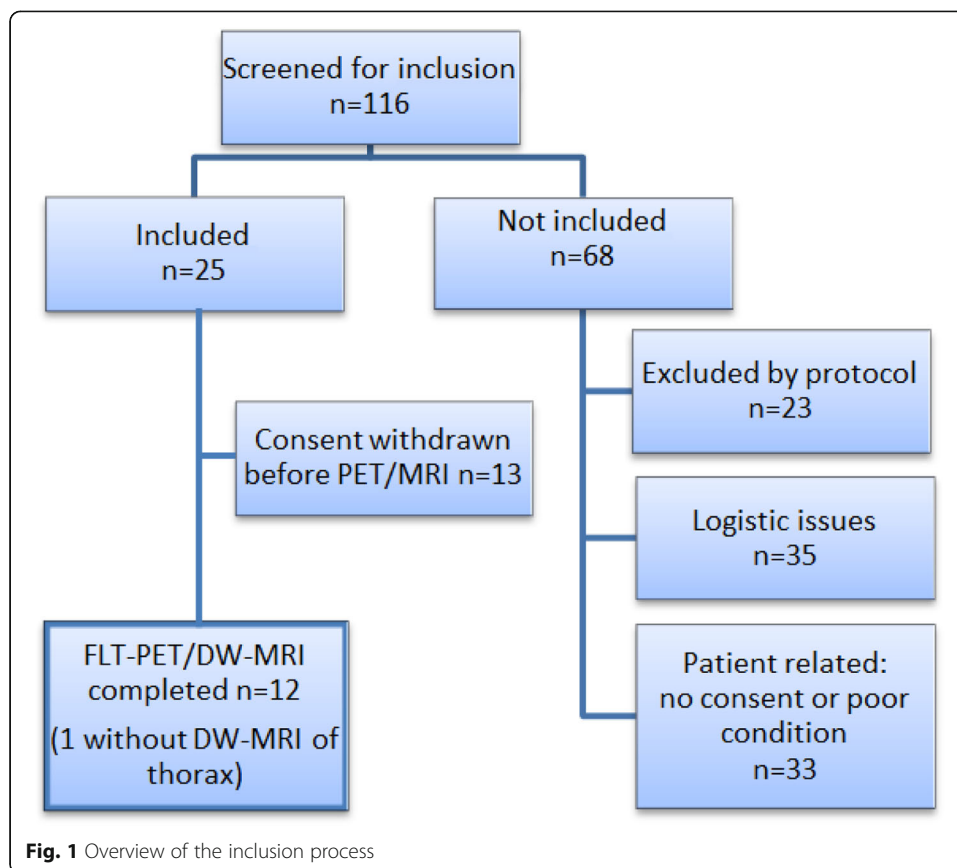
Correlation analyses of PET-parameters and MRI-parameters across patients were performed using Spearman's rank correlation. Within-patient voxel-by-voxel analyses were performed by linear regression.

Differences of each PET- and MRI-parameter in lesions with response vs. lesions with no change or progression were tested by an independent t test for response prediction. Levene's test was used for test of equality of variances and if variances were not equal; data was transformed by the natural logarithm prior to the independent t test analysis. PFS and OS were calculated using the Kaplan-Meier method. $P < 0.05$ was considered statistically significant.

Results

Patient data

FLT-PET/MRI was conducted in 12 patients, but in one patient, DW-MRI of thorax failed. Figure 1 provides an overview of the inclusion process. Table 1 presents the characteristics and outcome of the 12 patients. Nine patients had extensive disease (ED); one patient had limited disease (LD); and two patients had a relapse of SCLC and had previously been treated with concomitant chemo-radiotherapy. All patients were either active or former smokers with 40–60 pack-years.



All patients were treated with chemotherapy; 11 patients received at least three cycles of cis- or carboplatin and etoposide; one patient received only one cycle of etoposide. The patient with LD received concomitant radiotherapy (RT) to 45 Gy, and three patients with ED received sequential RT to 30 Gy; in two patients due to poor response to chemotherapy, and in one patient as consolidation treatment.

Median OS was 10.5 months, and median PFS was 5.1 months. Evaluated on CT, two patients had complete response, five patients had partial response, three patients had stable disease, one patient had progressive disease, and one patient had no relevant follow up scans as he died 1.5 months after treatment start. The seven responders all had relapse within 4 months after last exposure to chemotherapy.

Scan data

FLT-PET/MR was performed 1–9 days after start of chemotherapy (median 4.5 days). Pretreatment FDG-PET/CT was available in nine patients. FDG-PET/CT was performed 7–21 days before FLT-PET/DW-MRI (median 16 days). An overview of scan data and times is presented in Additional file 1: Table S1.

Malignant lesions

A total of 32 lesions were analyzed; 16 T-sites, 12 N-sites, and 4 M-sites. T-, N-, and M-sites will be described separately.

Table 1 Patient characteristics and outcome

Pt no.	Age	Sex	VALSG stage	PS	LDH	Treatment	Best response	PFS (days)	OS (days)	Follow up (days)
1	62	f	ED	1	220	Car+eto × 6	CR	246	349	
2	60	f	ED	1	231	Car+eto × 6 RT 30 Gy(bone metastases) PCI	PR	194	320	
3	72	m	ED	1	216	Car+eto × 6	PR	134	209	
4	77	m	ED	1	354	Car+eto × 3	SD	90	114	
5	59	f	ED/Relapse	2	267	Car+eto × 3	SD	220	220	
6	58	m	LD	0	172	Cis + eto × 2, car+eto × 2 Concomitant RT 60 Gy (RUL + mediastinum) PCI	CR	155		741
7	76	m	ED	3	1180	Eto × 1 RT (bone metastases)	NA*	47	47	
8	51	f	ED	1	160	Car+eto × 6 Sequential RT 30 Gy (mediastinum) PCI	PR	243		460
9	60	f	ED	1	264	Car+eto × 6	PR	195	321	
10	70	f	ED/Relapse	1	173	Car+eto × 3	PR	124	347	
11	59	m	ED	0	736	Car+eto × 6 Sequential RT 30 Gy (Right lung + mediastinum) RT 30 Gy (metastases on the thoracic wall and on skull)	SD	275	478	
12	74	m	ED	0	NA	Car+eto × 4 Sequential RT 30 Gy (mediastinum, neck)	PD	50	95	

f female, *m* male, *VALSG stage* The Veteran's administration Lung Study Group two stage classification scheme, *ED* extensive disease, *LD* limited disease, *PS* WHO performance status, *LDH* blood lactate dehydrogenase, *NA* not available, *car* carboplatin, *eto* etoposide, *RT* radiotherapy, *PCI* prophylactic cranial irradiation, *cis* cisplatin, *RUL* right upper lobe, *CR* complete response, *PR* partial response, *SD* stable disease, *PD* progressive disease, *PFS* progression free survival, *OS* overall survival; * No response evaluation, as the patient died prior to evaluation

Table 2 provides an overview of identified lesions, selected parameters, and lesion-specific outcome (all PET- and MRI-parameters are available in Additional file 2: Table S2). In many lesions, FLT-uptake was low compared with background uptake, and, accordingly, delineation of PTV was not possible in three of 16 T-sites and nine of 12 N-sites. Sufficient alignment was not achieved in all lesions and voxel-by-voxel analysis for FDG-PET vs. FLT-PET was feasible in only four T-sites, seven N-sites, and two M-sites. Voxel-by-voxel analyses for FLT-PET vs. DW-MRI were feasible in nine T-sites, nine N-sites, and two M-sites. The alignment of FDG-PET and DW-MRI was generally poor, and no voxel-by-voxel analyses of FDG-PET vs. ADC were feasible.

All SUVs from FDG-PET (FDG-SUV_{max}, FDG-SUV_{peak}, FDG-SUV_{mean41}, and FDG-SUV_{mean50}) were significantly correlated ($p < 0.001$), as were all SUVs from FLT-PET (FLT-SUV_{max}, FLT-SUV_{peak}, FLT-SUV_{mean41}, FLT-SUV_{mean50}, and FLT-SUV_{mean1.4}), all ADCs (ADC_{mean} and ADC_{median}), and all tumor volumes (MTV₄₁, MTV₅₀, PTV₄₁, PTV₅₀, PTV_{1.4}, DWTV₂₅, and GTV). Therefore, for further evaluation, only FDG-SUV_{peak}, FLT-SUV_{peak}, ADC_{median}, MTV₄₁, PTV₅₀, DWTV₂₅, TLG₄₁, and TLP₅₀ are presented.

Table 2 Malignant lesions: location, FDG-SUV_{peak}, FLT-SUV_{peak}, ADC_{median}, and outcome

Pt no	Lesion no	Location	FDG-PET	FLT-PET	DW-MRI	Lesion outcome		Comments
			SUV _{peak}	SUV _{peak}	ADC _{median}	Lesion response	Progression (days)	
1	1-T	LLL	16.5	1.6	1.22	Response	–	
	1-N1	2R + 4R	12.2	1.8	1.21	Response	–	
	1-N2	10L + 11L	13.4	1.5	0.90	Response	–	
	1-N3	4L	15.5	1.9	0.88	Response	–	
	1-N4	7	17.3	2.1	1.07	Response	–	
	1-M	RUL	4.2	1.1	1.05	Response	–	
2	2-N	2R + 4R + 4L + 7	NA	1.3	1.54	Response	194	
3	3-T	LLL + hilus sin	9.0	2.1	1.59	Response	–	
	3-N1	8	8.1	1.6	1.96	Response	–	
	3-N2	7	5.5	1.2	1.89	Response	–	
	3-N3	4L + 4R + 5	8.0	1.3	1.39	Response	134	
4	4-T	LUL	22.7	11.5	1.43	No change	90	
5	5-T	Hilus dxt	NA	2.6	1.74	No change	–	Previously irradiated
6	6-T	RLL	3.9	0.6	#	Response	155	
	6-N	10-11R	6.2	1.3	2.09	Response	–	
7	7-T	LUL + hilus + med	8.3	4.0	NA	NA	NA	No outcome evaluation as the patient died day 47
	7-M	Lymph node in left axilla	5.2	1.9	NA	NA	NA	No outcome evaluation as the patient died day 47
8	8-T1	RUL + med	9.7	1.7	1.11	Response	–	
	8-T2	RUL	2.0	0.6	#	Response	–	
	8-T3	RUL	2.2	0.7	#	Response	–	
9	9-T1	LUL + med	12.1	1.7	1.74	Response	195	
	9-T2	LUL	3.7	1.3	1.01	Response	–	
10	10-T1	hilus sin + med	NA	2.8	0.82	Response	124	Previously irradiated
	10-T2	lingula	NA	1.9	1.10	Response	–	
11	11-T1	RUL + med	11.8	3.0	1.15	No change	275	
	11-T2	RUL	4.4	1.0	0.76	NA	–	Response evaluation not possible due to atelectasis
	11-M1	Subcutis + os frontale	8.9	2.3	1.03	No change	–	
	11-M2	Subcutis + costa	10.9	4.6	1.03	No change	–	
12	12-T	RUL	12.8	1.2	1.19	Response	–	
	12-N1	4 + 7	11.6	2.4	1.56	Progression	50	
	12-N2	7 + 8	10.2	2.2	1.85	Progression	50	
	12-N3	10-11R	13.7	1.9	1.61	Progression	50	

LLL left lower lobe, RUL right upper lobe, 2R, 4R, etc lymph node stations, LUL left upper lobe, RLL right lower lobe; med: mediastinum, FDG ¹⁸F-fluorodeoxy-glucose, PET positron emission tomography, SUV standardized uptake value, FLT ¹⁸F-fluorothymidine, DW diffusion weighted, MRI magnetic resonance imaging, ADC apparent diffusion coefficient, NA not available, # Tumor not visible on MRI and/or DW-MRI

T-sites

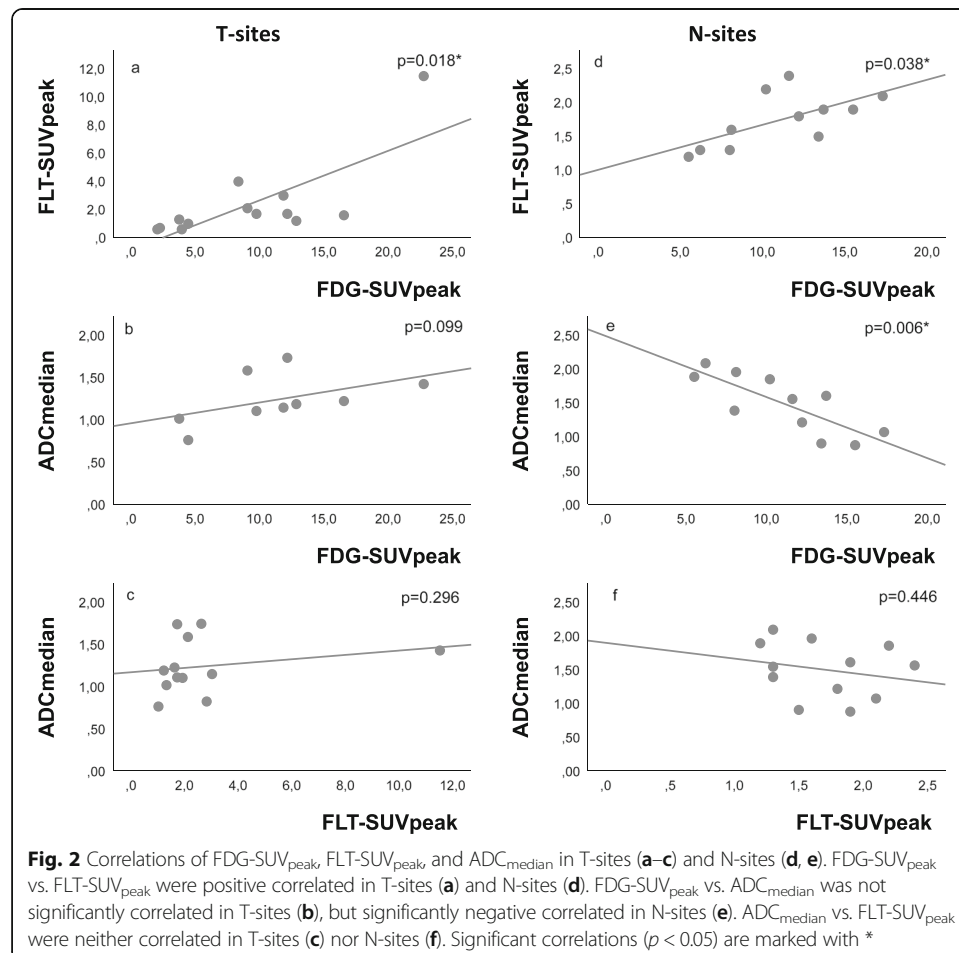
From the nine patients who had a pretreatment FDG-PET/CT, all T-sites ($n = 13$) were detectable by FDG-PET. $\text{FDG-SUV}_{\text{peak}}$ varied from 2.0 to 22.7.

All patients completed FLT-PET, but from the 16 T-sites, only five T-sites had an FLT-uptake clearly distinguishable from background. These five T-sites had a heterogeneous FLT-uptake and only a fraction of the tumor had a highly visible FLT-uptake. $\text{FLT-SUV}_{\text{peak}}$ from the 16 T-sites varied from 0.6 to 11.5.

From the 11 patients whom completed DW-MRI, 12 of 15 T-sites were detectable by DW-MRI, and $\text{ADC}_{\text{median}}$ varied from 0.76 to $1.74 \times 10^{-3} \text{ mm}^2/\text{s}$. Another three T-sites had no signal on DW-MRI: on pretreatment FDG-PET/CT, these were all small with a diameter of maximum 1.6 cm.

In each lesion, $\text{FLT-SUV}_{\text{peak}}$ was lower than $\text{FDG-SUV}_{\text{peak}}$. $\text{FDG-SUV}_{\text{peak}}$ and $\text{FLT-SUV}_{\text{peak}}$ were significantly correlated ($p = 0.018$), as shown in Fig. 2a. $\text{ADC}_{\text{median}}$ was not significantly correlated with $\text{FDG-SUV}_{\text{peak}}$ or $\text{FLT-SUV}_{\text{peak}}$, as shown in Fig. 2b, c.

Due to low FLT-uptake, limited spatial information was available in many lesions. Accordingly, comparison of the most “aggressive” regions on FDG-PET and FLT-PET were possible only in three T-sites. Within these three T-sites, the “aggressive” regions were distributed unevenly and there was no overlap of MTV70 and PTV70.



Voxel-by-voxel analysis comparing FDG-PET vs. FLT-PET was feasible in four T-sites. In three of four lesions, the overall voxel-by-voxel correlation of FDG-PET and FLT-PET was moderate ($r = 0.49\text{--}0.50$), but the voxels with highest FLT-uptake were randomly distributed along the FDG-uptake-scale, confirming that the overall correlation is not applicable for the hottest voxels. The fourth voxel-by-voxel analysis showed a weak correlation.

Comparison of the most “aggressive” regions of FLT-PET and DW-MRI was possible in four T-sites: Two T-sites had a partial overlap of PTV70 and DWTV50, and two T-sites had no overlap of PTV70 and DWTV50. There was no systematic correlation on the voxel-by-voxel analysis of FLT-PET and ADC ($r = -0.66$ to 0.42 , $n = 9$).

Figures 3 and 4 are examples of two representative T-sites with high, respectively, low FLT-uptake. As illustrated by Figs. 3 and 4, the three imaging modalities show apparently different patterns of intra-tumor heterogeneity.

N-sites

The 12 N-sites each consisted of a single lymph node or larger lymph node conglomerates, and therefore varied substantially in size (GTV: $3.9\text{--}119.7\text{ cm}^3$).

FDG-SUV_{peak} ranged from 5.5 to 17.3. FLT-uptake was distinguishable from background uptake only in three of 12 N-sites, all in the same patient. FLT-SUV_{peak} ranged from 1.2 to 2.4. ADC_{median} ranged from 0.88 to $2.09 \times 10^{-3}\text{ mm}^2/\text{s}$.

In each N-site, FLT-SUV_{peak} was lower than FDG-SUV_{peak}, and their correlation was significant ($p = 0.038$), see Fig. 2d. ADC_{median} correlated negative with FDG-SUV_{peak} ($p = 0.006$), but there was no significant correlation between ADC_{median} and FLT-SUV_{peak}, as illustrated in Fig. 2e, f.

Spatial comparisons were possible only in the three N-sites, due to the low detection rate by FLT-PET.

MTV70 and PTV70 showed partial or high overlap in all three N-sites, and voxel-by-voxel correlations of FDG-PET and FLT-PET was moderate and positive ($r = 0.41\text{--}0.60$). PTV70 and DWTV50 showed partial or high overlap, and voxel-by-voxel correlations of FLT-PET and ADC were weak and negative ($r = -0.44$ to -0.15).

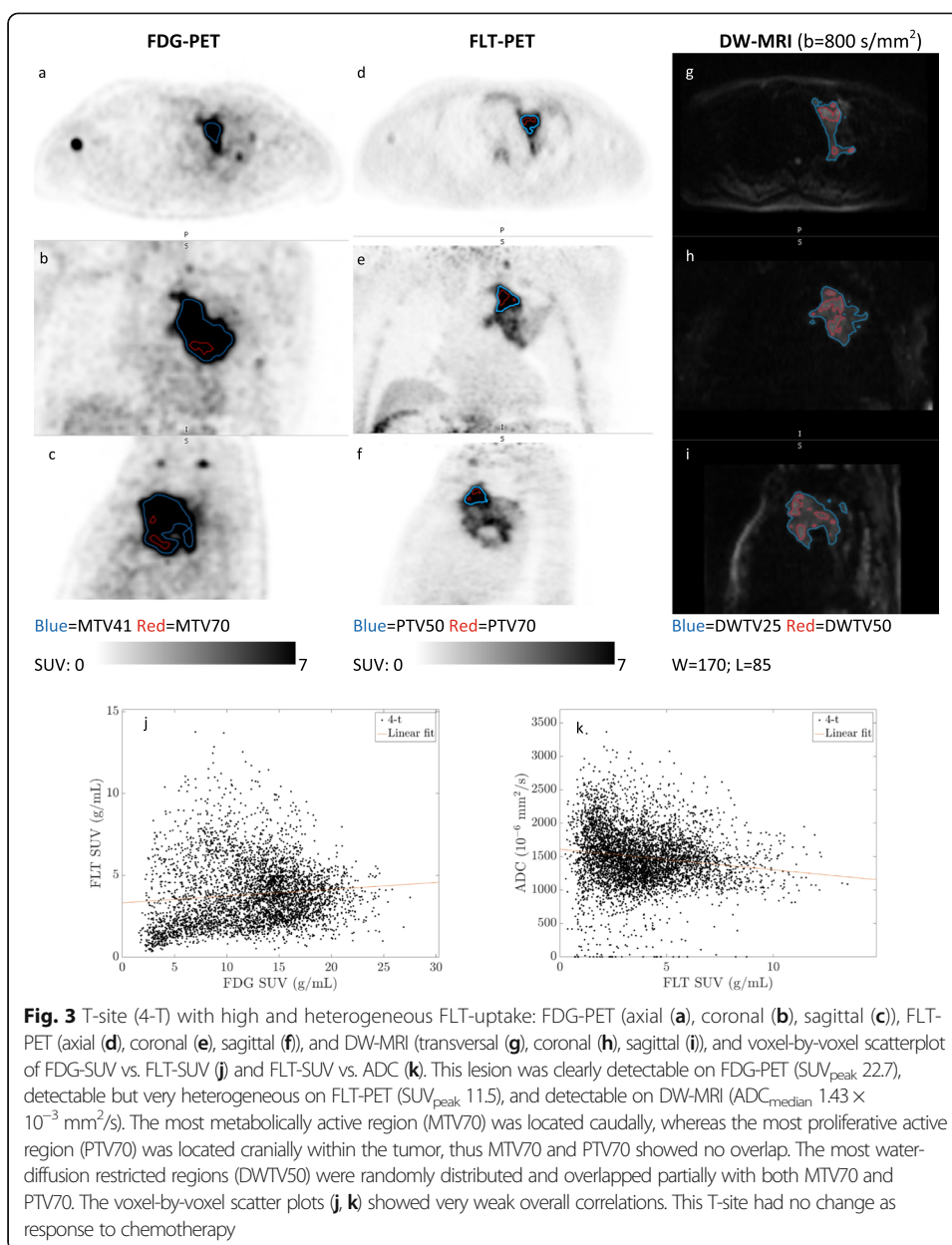
Figure 5 illustrates an N-site that could be visualized by all three imaging modalities. As illustrated with this N-site, but applicable for all three N-sites that were detectable by all three imaging modalities, the most “aggressive” regions showed partial or high overlap, but most lesions were undetectable by FLT-PET.

M-sites

No brain metastases were detected by FDG-PET, FLT-PET, DW-MRI, or MRI. M-sites were detected in the lung, in an axillary lymph node, two in subcutis, two in bones (vertebras), and several in the liver. Parameters from the four metastases in the lung, axilla, and subcutis are available in Table 2, but due to the small number and the heterogeneity of localization, no further analyses were conducted.

Prediction of final response to treatment

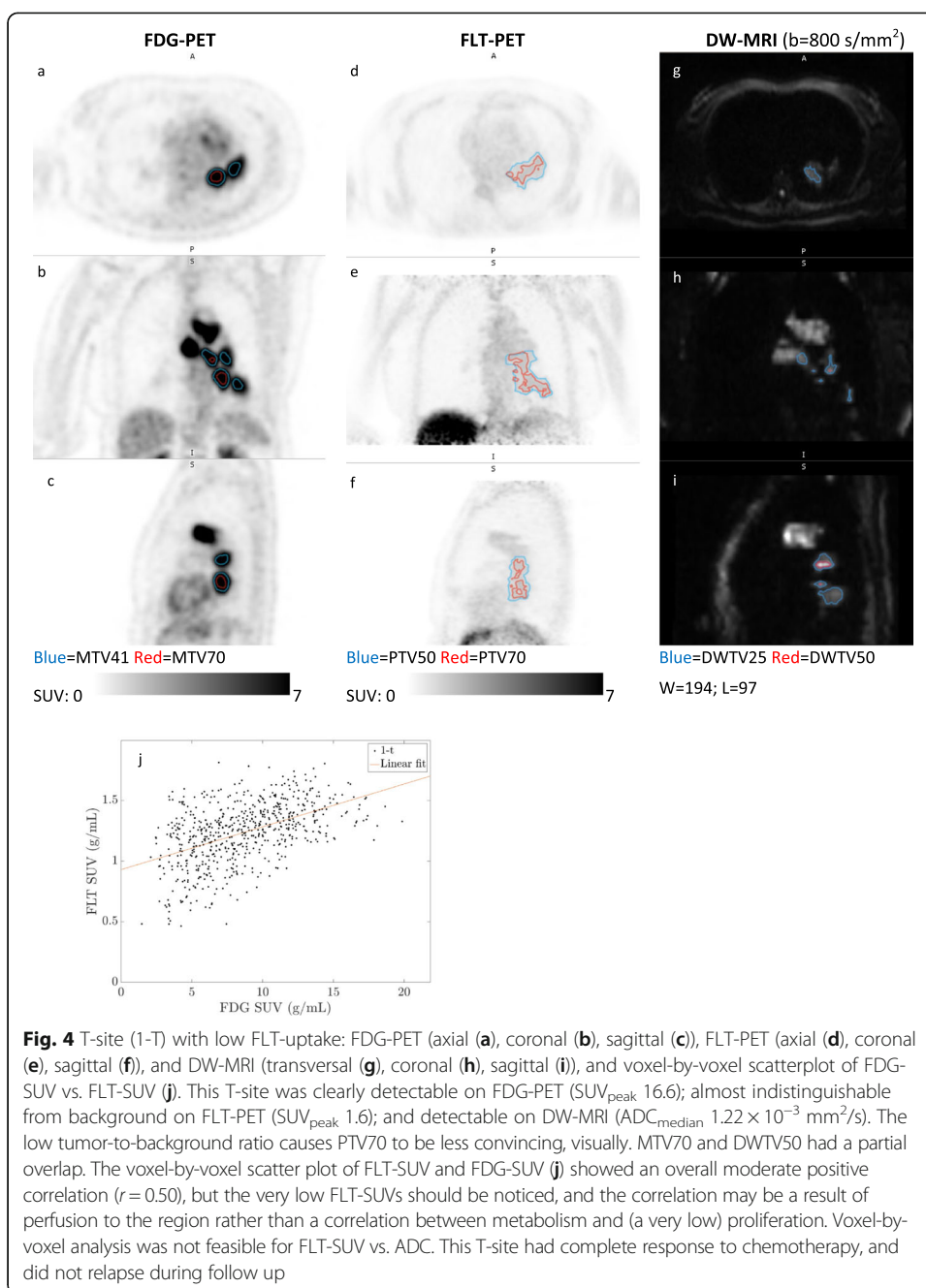
Of the 28 T- and N-sites, 20 responded to chemotherapy: three T-sites had no change and three N-sites progressed during chemotherapy. Another two lesions were not response evaluated; one because the patients died prior to evaluation (7-T); and one because it was incorporated in atelectasis and not evaluable after 6 cycles (11-T2).



No T-sites progressed during chemotherapy, and no N-sites had no change, therefore comparing analyses were performed of T-sites with response vs. no change, and N-sites with response vs. progression.

MTV41, TLG41, $FLT-SUV_{peak}$, and TLP50 were significantly lower in T-sites with response than T-sites with no change (mean MTV41: 41 vs. 208 cm^3 ; $p = 0.002$; mean TLG41: 311 vs. 2410; $p = 0.006$; mean $FLT-SUV_{peak}$: 1.5 vs. 5.7; $p = 0.007$; mean TLP50: 35.5 vs. 120.5; $p = 0.029$). In N-sites, $FLT-SUV_{peak}$ was significantly lower in responding N-sites than N-sites with progression (mean $FLT-SUV_{peak}$ 1.6 vs. 2.2; $p = 0.013$).

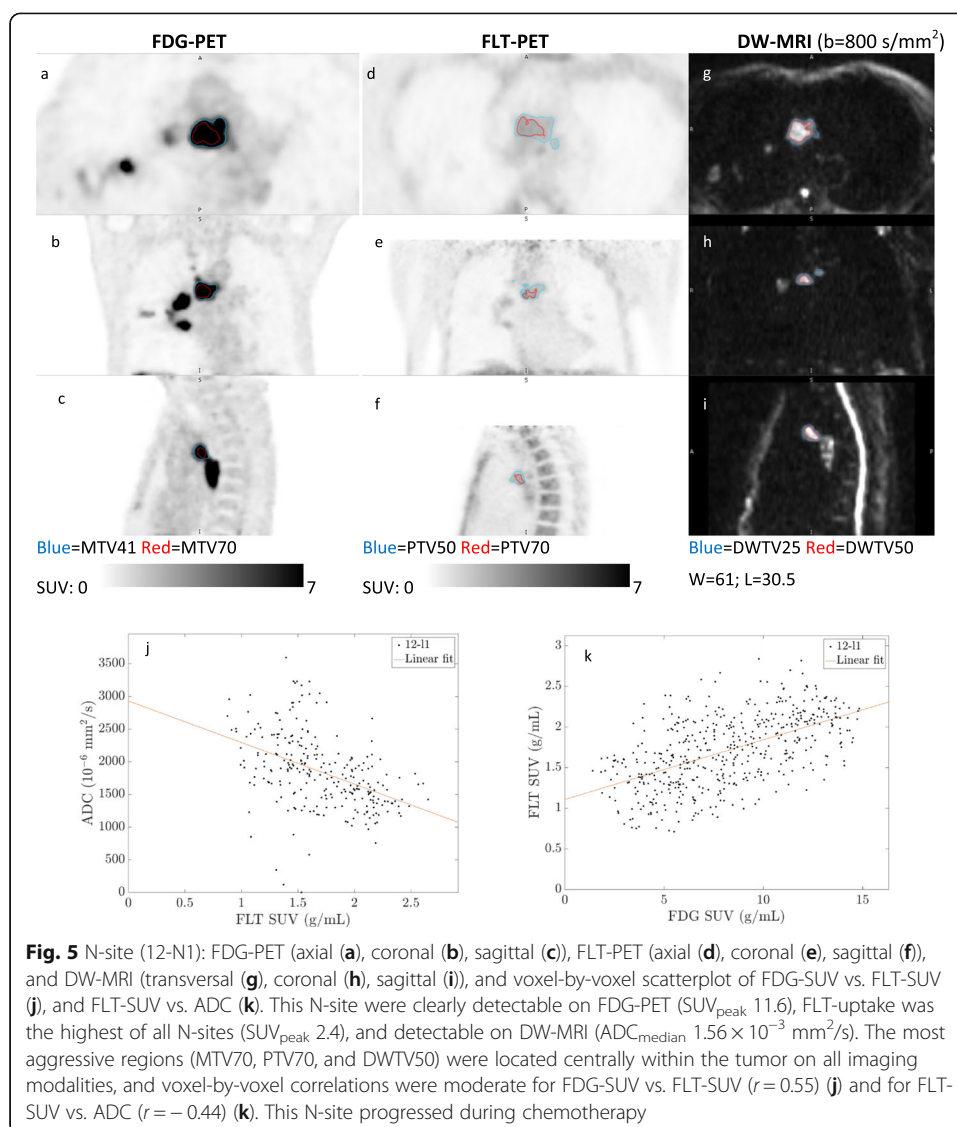
$FDG-SUV_{peak}$, TLG41, PTV50, ADC_{median} , and DWTV did not show any difference in responding vs. no change T-sites, or progressing N-sites, neither did MTV41 and TLP50 from N-sites.



The differences of $FDG-SUV_{peak}$, $FLT-SUV_{peak}$, and ADC_{median} in responding vs. no change or progressive lesions are illustrated in Fig. 6. As seen in Fig. 6b, $FLT-SUV_{peak}$ was lower in all, but one responding T-site ($FLT-SUV_{peak}$ 0.6–2.8) compared with T-sites with no change ($FLT-SUV_{peak}$ 2.6–11.5). All comparing analyses are available in Additional file 3: Table S3.

FLT uptake in normal tissue

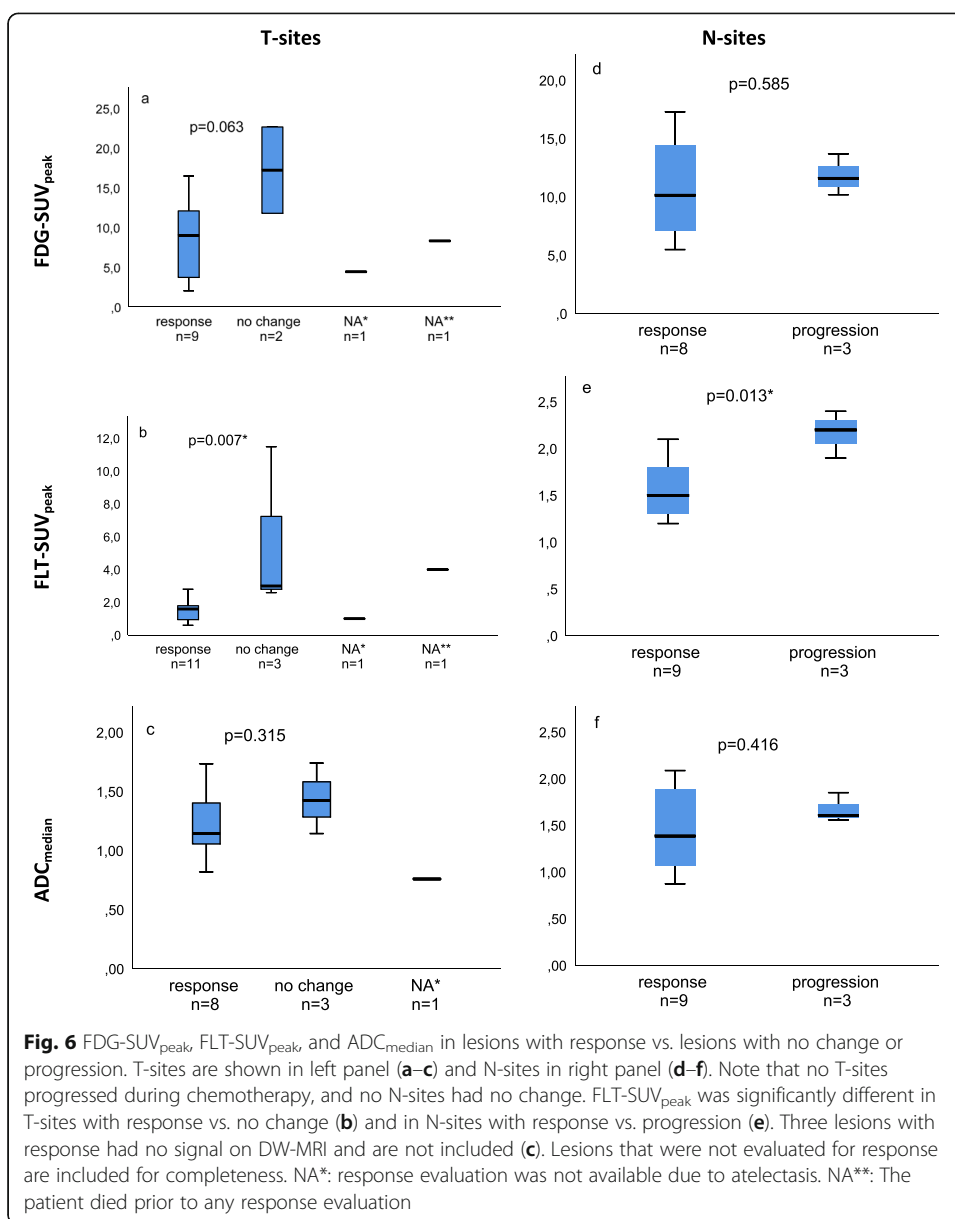
FLT-uptake in normal tissue showed large variation across the patients. Liver $FLT-SUV_{peak}$ ranged from 2.0 to 11.3 (reference: 3.46–7.46); blood pool $FLT-SUV_{peak}$



ranged from 0.6 to 1.3 (reference: 0.44–1.04); and bone marrow FLT- SUV_{peak} ranged from 1.2 to 11.3 (reference: 4.86–11.36), reference values from (Cysouw et al. 2017). There were no significant correlations between normal tissue FLT-uptake and time from treatment start to FLT-PET/MRI or FLT-uptake time. FLT-SUV in the liver, blood pool, and bone marrow are available in Additional file 4: Table S4. In most cases, FLT-uptake in normal tissue was not within Cysouw’s reference interval (Cysouw et al. 2017). In particular, bone marrow FLT-uptake was lower than the reference interval in ten of 12 patients. Three patients had a lower liver FLT-uptake compared with the reference interval, and two patients had higher liver and blood pool FLT-uptake compared with the reference interval.

Discussion

The aim of this study was to perform a pilot study of the potential of FLT-PET and DW-MRI early after treatment start in patients with small cell lung cancer. Our study indicates that FLT-PET and DW-MRI after one cycle of chemotherapy has a potential



to add biological information to pretreatment FDG-PET, as the most proliferative active regions measured by FLT-PET, the most water diffusion restricted regions measured by DW-MRI and the most metabolically active regions measured by FDG-PET were all dissimilarly distributed.

We showed that persistent proliferation measured by FLT-PET 1–9 days after start of chemotherapy is a potential predictor of non-response to treatment, whereas the value of DW-MRI early after treatment start was unconvincing as ADC was not associated with final response.

The secondary aim of our study was to examine the added value of FLT-PET/DW-MRI in detection of brain metastases from SCLC. Unfortunately, we were not able clarify this issue, as none of the included patients had brain metastases.

It has previously been reported that up to 40% of patients with ED SCLC do not achieve objective response to first line therapy (Lattuca-Truc et al. 2019); therefore, early response evaluation to identify non-responders may have great impact. CT-response after the first cycle of chemotherapy in patients with LD SCLC has shown prognostic value of PFS and OS (Halvorsen TO et al. 2016; Fujii et al. 2012; Lee et al. 2015), but whether early CT-response can predict final treatment response has not been addressed, and patients with ED were not included in these studies (Halvorsen TO et al. 2016; Fujii et al. 2012; Lee et al. 2015). FDG-PET/CT has shown potential of early response evaluation in two studies (Yamamoto et al. 2009; Fischer et al. 2006), but each study identified only one non-responder; therefore, the ability to discriminate between responders and non-responders were less powerful. In the present study, we showed that FLT-PET early after treatment start has a potential to predict final response. A cut-off was not established, but the overlap of FLT-SUV_{peak} in responding vs. non-responding lesions was small.

We did not find any potential value of DW-MRI early after treatment start in patients with SCLC. DW-MRI has only been investigated sparsely in patients with SCLC after treatment start. Tsuchida et al. (2013) included 11 patients with SCLC in a study of a mixed lung cancer cohort: ADC after treatment in patients with SCLC was similar to our results: $0.91\text{--}1.97 \times 10^{-3} \text{ mm}^2/\text{s}$, and absolute ADC after treatment was not associated with final response or OS. The change of ADC from baseline to early after treatment has shown predictive and prognostic value in patients with NSCLC (Weiss et al. 2016; Tsuchida et al. 2013; Yabuuchi et al. 2011; Yu et al. 2014). It seems ADC early after treatment start is less valuable than an ADC-change from baseline. The voxel-by-voxel correlations of FDG-PET, FLT-PET, and ADC were overall weak. Uncertainties of the intermodal image registration and varying respiration management strategies could potentially influence the voxel-by-voxel analysis. However, in consistence with the spatiovisual analysis, the results of the voxel-by-voxel analysis showed a dissimilar and heterogeneous distribution of the most aggressive regions of the modalities.

Recruiting patients to this study proved difficult and many potentially eligible patients were not included due to poor patient condition. To investigate the risk of a selection bias, we compared blood lactate dehydrogenase (LDH) and WHO performance status (PS) from a cohort of eligible, but not-included patients who attended our institution during the recruiting period and found no significant differences of LDH or PS (LDH: $p = 0.663$; PS: $p = 0.053$). Comparing our cohort with a recently published large French retrospective study of patients with SCLC from 1997 to 2017 (Lattuca-Truc et al. 2019), patients in our study had a better PS (PS ≥ 2 : 17% vs. 44%), but more often ED (92% vs. 58%), poorer response rate (63% vs. 73%), and slightly shorter OS (10.5 months vs. 12.2 months). A systematic bias in the recruiting process is therefore not obvious.

This study has several technical limitations. We included pretreatment FDG-PET/CTs conducted according to varying clinical protocols of several referring hospitals; accordingly, there were several technical variations from patient to patient, and the FDG-PET parameters should be interpreted with caution. FLT-PET/MRI was performed over cerebrum first and secondly over thorax, causing long FLT-uptake time before obtaining FLT-PET of thorax. MRI artifacts may affect the SUV quantification, as described in FDG-PET/MR (Olin et al. 2018). Reproducibility of FLT-SUV quantification after MRI attenuation correction has not been established, but for FDG-PET/MRI, the

reproducibility is high (Rasmussen et al. 2015). As a FLT-PET quality control, we assessed FLT-uptake in normal tissue for comparison with previously suggested references (Cysouw et al. 2017). In many cases, normal tissue FLT-uptake in our patients was not comprised within the reference intervals. In particular, bone marrow FLT-uptake was lower in ten of 12 patients, but also blood pool and liver FLT-uptake deviated from the references. The numerous outliers could have biological and/or technical explanations. Firstly, the known issue of detection of bone in Dixon MR-based attenuation (MRAC) correction may affect the measured FLT-uptake in the bone marrow as it is surrounded by bone (Samarin et al. 2012; Keller et al. 2013). Secondly, the reference intervals were established from a FLT-PET with a FLT-uptake time of 60 min, whereas FLT-uptake time in our study was 69–84 min. Thirdly, the PET reconstruction variables such as choice of reconstruction method (e.g., w/o time of flight and resolution modeling), number of iterations, and subsets and variations on correction methods (scatter, randoms and attenuation correction in general) can also influence PET quantification significantly. Noise in low FLT-uptake regions such as the blood pool and bone marrow might also have considerable effect. Fourthly, Cysouw's references was based on baseline imaging and based on patients treated with EGFR TKIs, and in this setting a slight increase in liver and bone marrow FLT-uptake after treatment was suggested. Our patients received a myelosuppressive treatment, and it has previously been shown that FLT-uptake in the bone marrow reflects the hematopoietic activity (Vercellino et al. 2017). In concordance with the lower bone marrow and liver FLT-uptake in our results, Leimgruber et al. found a decrease in liver and bone marrow FLT-uptake (median 31% and 22%, respectively) 2 weeks after treatment with cisplatin/etoposide in a concurrent radiotherapy regimen (Leimgruber et al. 2014). Fifthly, timing after treatment start may influence the effect of chemotherapy on normal tissue FLT-uptake. In our study, there was no significant correlation between the FLT-parameters and time from treatment start to FLT-PET/MR, but two patients in our study had FLT-PET/MRI conducted only 1 day after treatment start, and they both had higher FLT-uptake in the liver and in the blood pool than the remaining patients and higher than the references. It is plausible that different anticancer treatments affect proliferation in normal tissues differently, and the deviations of normal tissue FLT-uptake in this study from the references could solely originate from biologically induced changes. Despite the presence of technical limitations, we believe that the tendencies in this study are trustworthy.

With the recent introduction of new treatments, there is an urgent need for larger studies to determine the diagnostic accuracy and implication of early treatment response. Preclinical studies and studies of other cancers than SCLC have shown that FLT-SUV_{max} reduces more rapidly and/or more pronounced than FDG-SUV_{max} during therapy (Kahraman et al. 2012; Jensen et al. 2010; Mudd et al. 2012; Kishino et al. 2012), but individual treatments may affect FDG- and FLT-uptake changes differently (Jensen and Kjaer 2015), and thus should be investigated separately. In studies of NSCLC, esophagus cancer, and lymphoma, early response evaluated by FLT-PET predicted final response better than FDG-PET (Gerbaudo et al. 2018; Minamimoto et al. 2016; Everitt et al. 2014), but it is not clear whether response by FLT-PET has superior prognostic value to FDG-PET, as results have been inconsistent (Kahraman et al. 2012; Mileschkin et al. 2011; Everitt et al. 2017). FLT-PET early after treatment start is a

promising predictor for final response, but at this point, it is not clear which imaging modality is most valuable. For further validating the value of FLT-PET in SCLC, including baseline FLT-PET and correlating FDG-PET and FLT-PET at the same phase of treatments, would be beneficial in future studies.

Conclusions

Persistent proliferation measured by FLT-PET early after treatment start was associated with poor response to chemotherapy in patients with SCLC. Thus, FLT-PET is a potential tool for selecting patients to be considered for change of treatment. We found no association between DW-MRI early after treatment and the final response.

Supplementary information

Supplementary information accompanies this paper at <https://doi.org/10.1186/s41824-019-0071-5>.

Additional file 1: Table S1. Scan data and time points

Additional file 2: Table S2. PET- and MRI-parameters from malignant lesions

Additional file 3: Table S3. Comparison of PET- and MRI-parameters in lesions with response vs. no change or progression.

Additional file 4: Table S4. FLT-uptake in normal tissue.

Abbreviations

ADC: Apparent diffusion coefficient; DW-MRI: Diffusion-weighted magnetic resonance imaging; DWTV: Diffusion-weighted tumor volume; DWTV25 and DWTV50: Diffusion-weighted tumor volume delineated with thresholds of 25% and 50% of maximum, respectively; EANM: European Association of Nuclear Medicine; ED: Extensive disease; EGFR TKI: Epidermal growth factor receptor tyrosine kinase inhibitors; EPI: Echo-planar imaging; FDG: ^{18}F -fluorodeoxyglucose; FLT: ^{18}F -fluorothymidine; GTV: Gross tumor volume; LD: Limited disease; LDH: Lactate dehydrogenase; MRI: Magnetic resonance imaging; MTV: Metabolic tumor volume; MTV41, MTV50, and MTV70: Metabolic tumor volume delineated with thresholds of 41%, 50%, and 70% of SUV_{max} , respectively; NSCLC: Non-small cell lung cancer; OP-OSEM: Ordinary Poisson 3D ordered subset expectations maximization; OS: Overall survival; PET: Positron emission tomography; PFS: Progression-free survival; PS: Performance status; PTV: Proliferative tumor volume; PTV41, PTV50, PTV1.4, PTV70: Proliferative tumor volume delineated with thresholds of 40% of SUV_{max} , 50% of SUV_{max} , $\text{SUV} = 1.4$, and 70% of SUV_{max} , respectively; RECIST: The Response Evaluation Criteria in Solid Tumors; RT: Radiotherapy; SCLC: Small cell lung cancer; SUV: Standardized uptake value; SUV_{max} : Maximum standardized uptake value; $\text{SUV}_{\text{mean}41}$, $\text{SUV}_{\text{mean}50}$, and $\text{SUV}_{\text{mean}1.4}$: Mean of SUVs included in MTV41/PTV41, MTV50/PTV50, and PTV1.4, respectively; TE: Echo time; TLG: Total lesion glycolysis; TLP: Total lesion proliferation; TR: Repetition time

Acknowledgments

The authors thank all patients who participated in the study and staff at Dept. of Oncology and Dept. of Clinical Physiology, Nuclear Medicine and PET at Rigshospitalet for supporting the study. Thanks to John and Birthe Meyer Foundation for donating the PET/MRI to Rigshospitalet.

Author's contributions

Conception and design of the study: TNC, SWL, AK, BMF. Patient recruitment: TNC, SWL. PET/MRI-protocol set up: HHJ, JL, SHK, AEH. Data analysis and interpretation: TNC, SWL, KEV, HHJ, AEH, BMF. Manuscript preparation: TNC, BMF. All authors contributed to discussion of results and have read and approved the final manuscript.

Funding

This study was funded by Danish Cancer Society (grant no. R134-A8543–15-S42) and Dept. of Clinical Physiology, Nuclear Medicine and PET, Rigshospitalet, University of Copenhagen, Denmark.

Availability of data and materials

All datasets used during the current study are available from the corresponding author on reasonable request.

Ethics approval and consent to participate

This study was approved by The Committee on Health Research Ethics in The Capital Region of Denmark (approval number H-1-2014-026), and all patients gave written consent to participate.

Consent for publication

All patients gave written consent for publication.

Competing interests

The authors declare that they have no competing interests.

Author details

¹Department of Clinical Physiology, Nuclear Medicine & PET, Rigshospitalet, University of Copenhagen, Blegdamsvej 9, 2100 Copenhagen Ø, Denmark. ²Cluster for Molecular Imaging, University of Copenhagen, Copenhagen, Denmark. ³Department of Oncology, Rigshospitalet, University of Copenhagen, Copenhagen, Denmark. ⁴PET Centre, School of Biomedical Engineering and Imaging Science, Kings College London, London, UK.

Received: 4 September 2019 Accepted: 23 December 2019

Published online: 27 January 2020

References

- Aktan M, Koc M, Kanyilmaz G, Yavuz BB (2017) Prognostic value of pre-treatment (18)F-FDG-PET uptake in small-cell lung cancer. *Ann Nucl Med* 31(6):462–468
- Boellaard R, Delgado-Bolton R, Oyen WJ, Giammarile F, Tatsch K, Eschner W et al (2015) FDG PET/CT: EANM procedure guidelines for tumour imaging: version 2.0. *Eur J Nucl Med Mol Imaging* 42(2):328–354
- Brockenbrough JS, Souquet T, Morihara JK, Stern JE, Hawes SE, Rasey JS et al (2011) Tumor 3'-deoxy-3'-(18)F-fluorothymidine ((18)F-FLT) uptake by PET correlates with thymidine kinase 1 expression: static and kinetic analysis of (18)F-FLT PET studies in lung tumors. *J Nucl Med* 52(8):1181–1188
- Chang H, Lee SJ, Lim J, Lee JS, Kim YJ, Lee WW (2019) Prognostic significance of metabolic parameters measured by (18)F-FDG PET/CT in limited-stage small-cell lung carcinoma. *J Cancer Res Clin Oncol* 145(5):1361–1367
- Crandall JP, Tahari AK, Juergens RA, Brahmer JR, Rudin CM, Esposito G et al (2017) A comparison of FLT to FDG PET/CT in the early assessment of chemotherapy response in stages IB-IIIa resectable NSCLC. *EJNMMI Res* 7(1):8
- Cysouw MCF, Kramer GM, Frings V, De Langen AJ, Wondergem MJ, Kenny LM et al (2017) Baseline and longitudinal variability of normal tissue uptake values of [(18)F]-fluorothymidine-PET images. *Nucl Med Biol* 51:18–24
- Dayen C, Debievre D, Molinier O, Raffy O, Paganin F, Virally J et al (2017) New insights into stage and prognosis in small cell lung cancer: an analysis of 968 cases. *J Thorac Dis* 9(12):5101–5111
- Dittmann H, Dohmen BM, Paulsen F, Eichhorn K, Eschmann SM, Horger M et al (2003) [18F] FLT PET for diagnosis and staging of thoracic tumours. *Eur J Nucl Med Mol Imaging* 30(10):1407–1412
- Eisenhauer EA, Therasse P, Bogaerts J, Schwartz LH, Sargent D, Ford R et al (2009) New response evaluation criteria in solid tumours: revised RECIST guideline (version 1.1). *Eur J Cancer* 45(2):228–247
- Everitt S, Ball D, Hicks RJ, Callahan J, Plumridge N, Trinh J et al (2017) Prospective study of serial imaging comparing fluorodeoxyglucose positron emission tomography (PET) and fluorothymidine PET during radical chemoradiation for non-small cell lung cancer: reduction of detectable proliferation associated with worse survival. *Int J Radiat Oncol Biol Phys* 99(4):947–955
- Everitt SJ, Ball DL, Hicks RJ, Callahan J, Plumridge N, Collins M et al (2014) Differential (18)F-FDG and (18)F-FLT uptake on serial PET/CT imaging before and during definitive chemoradiation for non-small cell lung cancer. *J Nucl Med* 55(7):1069–1074
- Fischer BM, Mortensen J, Langer SW, Loft A, Berthelsen AK, Daugaard G et al (2006) PET/CT imaging in response evaluation of patients with small cell lung cancer. *Lung Cancer* 54(1):41–49
- Fu L, Zhu Y, Jing W, Guo D, Kong L, Yu J (2018) Incorporation of circulating tumor cells and whole-body metabolic tumor volume of (18)F-FDG PET/CT improves prediction of outcome in IIIB stage small-cell lung cancer. *Chin J Cancer Res* 30(6):596–604
- Fujii M, Hotta K, Takigawa N, Hisamoto A, Ichihara E, Tabata M et al (2012) Influence of the timing of tumor regression after the initiation of chemoradiotherapy on prognosis in patients with limited-disease small-cell lung cancer achieving objective response. *Lung Cancer* 78(1):107–111
- Gerbaudo VH, Killoran JH, Kim CK, Hornick JL, Nowak JA, Enzinger PC et al (2018) Pilot study of serial FLT and FDG-PET/CT imaging to monitor response to neoadjuvant chemoradiotherapy of esophageal adenocarcinoma: correlation with histopathologic response. *Ann Nucl Med* 32(3):165–174
- Halvorsen TO, Herje M, Levin N, Bremnes RM, Brustugun OT, Flotten O et al (2016) Tumour size reduction after the first chemotherapy-course and outcomes of chemoradiotherapy in limited disease small-cell lung cancer. *Lung Cancer* 102:9–14
- Horn L, Mansfield AS, Szczesna A, Havel L, Krzakowski M, Hochmair MJ et al (2018) First-line Atezolizumab plus chemotherapy in extensive-stage small-cell lung cancer. *N Engl J Med* 379(23):2220–2229
- Hoshikawa H, Kishino T, Mori T, Nishiyama Y, Yamamoto Y, Mori N (2013) The value of 18F-FLT PET for detecting second primary cancers and distant metastases in head and neck cancer patients. *Clin Nucl Med* 38(8):e318–e323
- Jensen MM, Erichsen KD, Bjorkling F, Madsen J, Jensen PB, Hojgaard L et al (2010) Early detection of response to experimental chemotherapeutic Top216 with [18F] FLT and [18F] FDG PET in human ovary cancer xenografts in mice. *PLoS One* 5(9):e12965
- Jensen MM, Kjaer A (2015) Monitoring of anti-cancer treatment with (18)F-FDG and (18)F-FLT PET: a comprehensive review of pre-clinical studies. *Am J Nucl Med Mol Imaging* 5(5):431–456
- Kahraman D, Holstein A, Scheffler M, Zander T, Nogova L, Lammertsma AA et al (2012) Tumor lesion glycolysis and tumor lesion proliferation for response prediction and prognostic differentiation in patients with advanced non-small cell lung cancer treated with erlotinib. *Clin Nucl Med* 37(11):1058–1064
- Kahraman D, Scheffler M, Zander T, Nogova L, Lammertsma AA, Boellaard R et al (2011) Quantitative analysis of response to treatment with erlotinib in advanced non-small cell lung cancer using 18F-FDG and 3'-deoxy-3'-18F-fluorothymidine PET. *J Nucl Med* 52(12):1871–1877
- Keller SH, Holm S, Hansen AE, Sattler B, Andersen F, Klausen TL et al (2013) Image artifacts from MR-based attenuation correction in clinical, whole-body PET/MRI. *MAGMA*. 26(1):173–181
- Kim H, Yoo IR, Boo SH, Park HL, OJH KSH (2018) Prognostic value of pre- and post-treatment FDG PET/CT parameters in small cell lung Cancer patients. *Nucl Med Mol Imaging* 52(1):31–38
- Kishino T, Hoshikawa H, Nishiyama Y, Yamamoto Y, Mori N (2012) Usefulness of 3'-deoxy-3'-18F-fluorothymidine PET for predicting early response to chemoradiotherapy in head and neck cancer. *J Nucl Med* 53(10):1521–1527

- Langer NH, Christensen TN, Langer SW, Kjaer A, Fischer BM (2014) PET/CT in therapy evaluation of patients with lung cancer. *Expert Rev Anticancer Ther* 14(5):595–620
- Lattuca-Truc M, Timsit JF, Levra MG, Ruckly S, Villa J, Dumas I et al (2019) Trends in response rate and survival in small-cell lung cancer patients between 1997 and 2017. *Lung Cancer* 131:122–127
- Lee J, Kim JO, Jung CK, Kim YS, Yoo le R, Choi WH et al (2014) Metabolic activity on [18F]-fluorodeoxyglucose-positron emission tomography/computed tomography and glucose transporter-1 expression might predict clinical outcomes in patients with limited disease small-cell lung cancer who receive concurrent chemoradiation. *Clin Lung Cancer* 15(2):e13–e21
- Lee J, Lee J, Choi J, Kim JW, Cho J, Lee CG (2015) Early treatment volume reduction rate as a prognostic factor in patients treated with chemoradiotherapy for limited stage small cell lung cancer. *Radiat Oncol J* 33(2):117–125
- Leimgruber A, Moller A, Everitt SJ, Chabrot M, Ball DL, Solomon B et al (2014) Effect of platinum-based chemoradiotherapy on cellular proliferation in bone marrow and spleen, estimated by (18)F-FLT PET/CT in patients with locally advanced non-small cell lung cancer. *J Nucl Med* 55(7):1075–1080
- Luis G, JMTP P-A, Besse B, Moreno V, Lopez R, Sala MA et al (2019) Efficacy and safety profile of lurbinectedin in second-line SCLC patients: results from a phase II single-agent trial. *J Clin Oncol* 37:suppl; abstr 8506
- Mileshkin L, Hicks RJ, Hughes BG, Mitchell PL, Charu V, Gitlitz BJ et al (2011) Changes in 18F-fluorodeoxyglucose and 18F-fluorodeoxythymidine positron emission tomography imaging in patients with non-small cell lung cancer treated with erlotinib. *Clin Cancer Res* 17(10):3304–3315
- Minamimoto R, Fayad L, Advani R, Vose J, Macapinlac H, Meza J et al (2016) Diffuse large B-cell lymphoma: prospective multicenter comparison of early interim FLT PET/CT versus FDG PET/CT with IHP, EORTC, Deauville, and PERCIST criteria for early therapeutic monitoring. *Radiology*. 280(1):220–229
- Mirili C, Guney IB, Paydas S, Seydaoglu G, Kapukaya TK, Ogul A et al (2019) Prognostic significance of neutrophil/lymphocyte ratio (NLR) and correlation with PET-CT metabolic parameters in small cell lung cancer (SCLC). *Int J Clin Oncol* 24(2):168–178
- Mudd SR, Holich KD, Voorbach MJ, Cole TB, Reuter DR, Tapang P et al (2012) Pharmacodynamic evaluation of irinotecan therapy by FDG and FLT PET/CT imaging in a colorectal cancer xenograft model. *Mol Imaging Biol* 14(5):617–624
- Nakajo M, Nakajo M, Jinguji M, Tani A, Kajiya Y, Tanabe H et al (2013) Diagnosis of metastases from postoperative differentiated thyroid cancer: comparison between FDG and FLT PET/CT studies. *Radiology*. 267(3):891–901
- Nestle U, De Ruysscher D, Ricardi U, Geets X, Belderbos J, Pottgen C et al (2018) ESTRO ACROP guidelines for target volume definition in the treatment of locally advanced non-small cell lung cancer. *Radiother Oncol* 127(1):1–5
- Nguyen NC, Yee MK, Tuchayi AM, Kirkwood JM, Tawbi H, Mountz JM (2018) Targeted therapy and immunotherapy response assessment with F-18 Fluorothymidine positron-emission tomography/magnetic resonance imaging in melanoma brain metastasis: a pilot study. *Front Oncol* 8:18
- Nikaki A, Angelidis G, Efthimiadou R, Tsougos I, Valotassiou V, Fountas K et al (2017) (18)F-fluorothymidine PET imaging in gliomas: an update. *Ann Nucl Med* 31(7):495–505
- Olin A, Ladefoged CN, Langer NH, Keller SH, Lofgren J, Hansen AE et al (2018) Reproducibility of MR-based attenuation maps in PET/MRI and the impact on PET quantification in lung cancer. *J Nucl Med* 59(6):999–1004
- Pardo OE, Latigo J, Jeffery RE, Nye E, Poulsom R, Spencer-Dene B et al (2009) The fibroblast growth factor receptor inhibitor PD173074 blocks small cell lung cancer growth in vitro and in vivo. *Cancer Res* 69(22):8645–8651
- Park SB, Choi JY, Moon SH, Yoo J, Kim H, Ahn YC et al (2014) Prognostic value of volumetric metabolic parameters measured by [18F]fluorodeoxyglucose-positron emission tomography/computed tomography in patients with small cell lung cancer. *Cancer Imaging* 14:2
- Rasmussen JH, Fischer BM, Aznar MC, Hansen AE, Vogelius IR, Lofgren J et al (2015) Reproducibility of (18)F-FDG PET uptake measurements in head and neck squamous cell carcinoma on both PET/CT and PET/MR. *Br J Radiol* 88(1048):20140655
- Ready N, Farago AF, de Braud F, Atmaca A, Hellmann MD, Schneider JG et al (2018) Third-line Nivolumab Monotherapy in recurrent small cell lung cancer: CheckMate 032. *J Thorac Oncol* 14(2):237–244
- Ruben JD, Ball DL (2012) The efficacy of PET staging for small-cell lung cancer: a systematic review and cost analysis in the Australian setting. *J Thorac Oncol* 7(6):1015–1020
- Samarin A, Burger C, Wollenweber SD, Crook DW, Burger IA, Schmid DT et al (2012) PET/MR imaging of bone lesions—implications for PET quantification from imperfect attenuation correction. *Eur J Nucl Med Mol Imaging* 39(7):1154–1160
- Shen G, Jia Z, Deng H (2016) Apparent diffusion coefficient values of diffusion-weighted imaging for distinguishing focal pulmonary lesions and characterizing the subtype of lung cancer: a meta-analysis. *Eur Radiol* 26(2):556–566
- Sohn HJ, Yang YJ, Ryu JS, Oh SJ, Im KC, Moon DH et al (2008) [18F] Fluorothymidine positron emission tomography before and 7 days after gefitinib treatment predicts response in patients with advanced adenocarcinoma of the lung. *Clin Cancer Res* 14(22):7423–7429
- Thureau S, Chaumet-Riffaud P, Modzelewski R, Fernandez P, Tessonnier L, Vervueren L et al (2013) Interobserver agreement of qualitative analysis and tumor delineation of 18F-fluoromisonidazole and 3'-deoxy-3'-18F-fluorothymidine PET images in lung cancer. *J Nucl Med* 54(9):1543–1550
- Trigonis I, Koh PK, Taylor B, Tamal M, Ryder D, Earl M et al (2014) Early reduction in tumour [18F] fluorothymidine (FLT) uptake in patients with non-small cell lung cancer (NSCLC) treated with radiotherapy alone. *Eur J Nucl Med Mol Imaging* 41(4):682–693
- Tsuchida T, Morikawa M, Demura Y, Umeda Y, Okazawa H, Kimura H (2013) Imaging the early response to chemotherapy in advanced lung cancer with diffusion-weighted magnetic resonance imaging compared to fluorine-18 fluorodeoxyglucose positron emission tomography and computed tomography. *J Magn Reson Imaging* 38(1):80–88
- Usuda K, Funasaki A, Sekimura A, Motono N, Matoba M, Doai M et al (2018) FDG-PET/CT and diffusion-weighted imaging for resected lung cancer: correlation of maximum standardized uptake value and apparent diffusion coefficient value with prognostic factors. *Med Oncol* 35(5):66
- van Loon J, van Baardwijk A, Boersma L, Ollers M, Lambin P, De Ruysscher D (2011) Therapeutic implications of molecular imaging with PET in the combined modality treatment of lung cancer. *Cancer Treat Rev* 37(5):331–343
- Vercellino L, Ouvrier MJ, Barre E, Cassinat B, de Beco V, Dosquet C et al (2017) Assessing bone marrow activity in patients with myelofibrosis: results of a pilot study of (18)F-FLT PET. *J Nucl Med* 58(10):1603–1608

- Weiss E, Ford JC, Olsen KM, Karki K, Saraiya S, Groves R et al (2016) Apparent diffusion coefficient (ADC) change on repeated diffusion-weighted magnetic resonance imaging during radiochemotherapy for non-small cell lung cancer: a pilot study. *Lung Cancer* 96:113–119
- Yabuuchi H, Hatakenaka M, Takayama K, Matsuo Y, Sunami S, Kamitani T et al (2011) Non-small cell lung cancer: detection of early response to chemotherapy by using contrast-enhanced dynamic and diffusion-weighted MR imaging. *Radiology*. 261(2):598–604
- Yamamoto Y, Kameyama R, Murota M, Bandoh S, Ishii T, Nishiyama Y (2009) Early assessment of therapeutic response using FDG PET in small cell lung cancer. *Mol Imaging Biol* 11(6):467–472
- Yap CS, Czernin J, Fishbein MC, Cameron RB, Schiepers C, Phelps ME et al (2006) Evaluation of thoracic tumors with 18F-fluorothymidine and 18F-fluorodeoxyglucose-positron emission tomography. *Chest*. 129(2):393–401
- Yu J, Li W, Zhang Z, Yu T, Li D (2014) Prediction of early response to chemotherapy in lung cancer by using diffusion-weighted MR imaging. *TheScientificWorldJournal*. 2014:135841

Publisher's Note

Springer Nature remains neutral with regard to jurisdictional claims in published maps and institutional affiliations.

Submit your manuscript to a SpringerOpen[®] journal and benefit from:

- ▶ Convenient online submission
- ▶ Rigorous peer review
- ▶ Open access: articles freely available online
- ▶ High visibility within the field
- ▶ Retaining the copyright to your article

Submit your next manuscript at ▶ [springeropen.com](https://www.springeropen.com)
